Structural Biology

International Edition: DOI: 10.1002/anie.201609617
German Edition: DOI: 10.1002/ange.201609617

Long Distance Measurements up to 160 Å in the GroEL Tetradecamer Using Q-Band DEER EPR Spectroscopy

*Thomas Schmidt, Marielle A. Wälti, James L. Baber, Eric J. Hustedt, and G. Marius Clore**

Abstract: *Current distance measurements between spin-labels on multimeric protonated proteins using double electron–electron resonance (DEER) EPR spectroscopy are generally limited to the 15–60 Å range. Here we show how DEER experiments can be extended to dipolar evolution times of ca. 80 μs, permitting distances up to 170 Å to be accessed in multimeric proteins. The method relies on sparse spin-labeling, supplemented by deuteration of protein and solvent, to minimize the deleterious impact of multispin effects and substantially increase the apparent spin-label phase memory relaxation time, complemented by high sensitivity afforded by measurements at Q-band. We demonstrate the approach using the tetradecameric molecular machine GroEL as an example. Two engineered surface-exposed mutants, R268C and E315C, are used to measure pairwise distance distributions with mean values ranging from 20 to 100 Å and from 30 to 160 Å, respectively, both within and between the two heptameric rings of GroEL. The measured distance distributions are consistent with the known crystal structure of apo GroEL. The methodology presented here should significantly expand the use of DEER for the structural characterization of conformational changes in higher order oligomers.*

Double electron–electron resonance (DEER) EPR spectroscopy[1] offers a powerful method of probing conformational changes in biological macromolecules by measuring quantitative distances between pairs of spin labels.[2] Typically, distances within the range 15–60 Å for protonated proteins and up to 90 Å for deuterated proteins are accessible by DEER.[2c,3] Symmetric multimeric proteins, however, present a particular challenge for the quantitative interpretation of DEER data, owing to the negative impact of multispin effects which arise when three or more spin labels are located in close proximity.[2c,4] The phase memory relaxation time, T_m, which dictates the length of the dipolar coupling evolution time in a DEER experiment and hence both the accessible distance range and signal-to-noise, decreases as the number of spins within a particular molecular assembly increases.[4d,5] Further, the presence of more than two spins results in so-called "ghost peaks" in the DEER-derived distance distributions owing to higher-order sum and difference dipolar frequency contributions to the DEER echo curve.[6] In this paper we present a simple approach employing sparse spin-labeling that can circumvent the deleterious impact of multispin effects. We demonstrate distance measurements of 160 Å using the molecular machine GroEL comprising 14 identical subunits arranged in two stacked heptameric rings (Figure 1).[7]

In these studies, two engineered, surface-exposed cysteine mutants of GroEL were employed: R268C and E315C. For

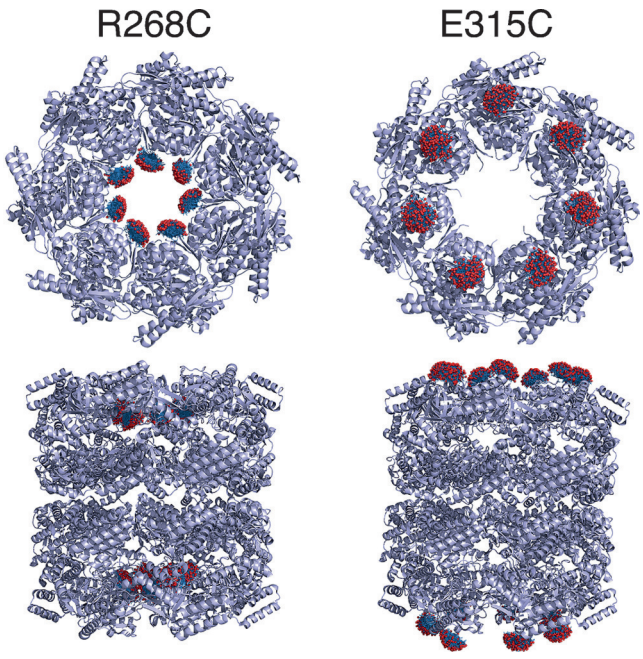

Figure 1. GroEL spin-labeling. Ribbon diagrams of apo GroEL (PDB 1XCK)[8] showing a single heptameric ring (top) and two stacked heptameric rings (bottom) viewed orthogonal and parallel, respectively, to the long axis of the cavity, illustrating the positions of the spin-labels (oxygen, red spheres; other atoms, blue bonds) for R268C (left panel) and E315C (right panel). The program SCWRL4.0[9] was used to optimize side chain positions before loading the coordinates into the MMMv2013.2[10] program to generate rotamer probabilities for the spin-labels. In these studies, two engineered, surface-exposed cysteine mutants of GroEL were employed: R268C and E315C. (Further details of protein expression, purification, nitroxide spin-labeling and sample preparation are provided in the SI.) For any given spin label, there are 6 intra-ring and 7 inter-ring spin pairs. The pairwise distances between spin-labels, calculated from the crystal structure (PDB 1XCK)[8] using the program MMMv2013.2,[10] range from 15 to 80 Å within a heptameric ring, and from 90 to 170 Å between rings. The latter encompass a broad range of distributions centred about 100 Å and 160 Å for the R268C and E315C constructs of GroEL, respectively.

[*] Dr. T. Schmidt, Dr. M. A. Wälti, Dr. J. L. Baber, Dr. G. M. Clore
Laboratory of Chemical Physics, National Institutes of Diabetes and Digestive and Kidney Diseases, National Institutes of Health
Bethesda, MD 20892-0520 (USA)
E-mail: mariusc@mail.nih.gov
Dr. E. J. Hustedt
Department of Molecular Physiology and Biophysics, Vanderbilt University, Nashville, TN 37232 (USA)

Supporting information and the ORCID identification number(s) for the author(s) of this article can be found under http://dx.doi.org/10.1002/anie.201609617.

any given spin label, there are 6 intra-ring and 7 inter-ring spin pairs (Figure 1). The distances between spin-labels, calculated from the crystal structure (PDB 1XCK)[8] using the program MMMv2013.2,[10] range from 15 to 80 Å within a heptameric ring, and from 90 to 170 Å between rings. The latter encompass a broad range of distributions centred about 100 Å and 160 Å for the R268C and E315C constructs of GroEL, respectively. The room temperature X-band CW spectrum for nitroxide spin-labeled GroEL(E315C) is characterized by relatively narrow linewidths indicative of mobile spin labels[11] (see the Supporting Information (SI), Figure S1 A); that for GroEL(R268C), however, appears broad (SI Figure S1 A) despite the fact that a wide range of rotamers is predicted for both spin-labels by MMMv2013.2[10] (Figure 1). This is due to the fact that for the R268C construct (but not the E315C construct) there are pairs of spin labels within a heptameric ring separated by less than 15 Å. These short distances result in strong dipolar interactions that broaden the EPR spectrum, as confirmed by the Q-band echo-detected EPR spectrum (SI Figure S1 B).

In the four-pulse DEER experiment,[1d] the reliability of the $P(r)$ distance distribution is governed by the maximum dipolar evolution time, t_{max}.[2c] For $t_{max} = 2$ µs, reliable distances can be obtained up to 50 Å, and this limit scales as $t_{max}^{1/3}$.[2c] Thus, t_{max} values of 20 and 80 µs would be required to accurately determine distances of approximately 100 and 170 Å, respectively. In the literature t_{max} is usually only extended out to ca. 1.5 T_m to obtain adequate sensitivity.[3a] As a result, such long t_{max} values are generally precluded since T_m values are typically of a few microseconds or less in protonated protein samples. Deuteration of both protein and solvent can significantly extend the T_m by removing electron–nuclear dipole interactions between spin labels and nearby protons.[3b,12] This is illustrated by the spin-echo decay curve for a model system comprising doubly spin-labeled, deuterated, monomeric protein A[12] shown in SI Figure S2 ($T_m \sim 64$ µs) which clearly shows that DEER data can easily be acquired to $t_{max} = 80$ µs in a simple two spin system. For a multispin system, however, deuteration alone is entirely insufficient, as shown by the spin-echo decay curve for deuterated GroEL(E315C) in which every subunit is spin-labeled (i.e. a total of 14 spin labels): a bi-exponential decay is observed with fast ($T_m^{fast} \sim 1.5$ µs) and slow ($T_m^{slow} \sim 18$ µs) components arising from spin–spin relaxation between dipole-coupled spin labels and various forms of spin diffusion (black trace in Figure 2 A). Further, the amplitude of the fast component is very high (ca. 70 %; cf. Table 1) precluding the use of t_{max} values much larger than about 2.5 to 3 µs in a DEER experiment, corresponding to an upper distance of ca. 60 Å, in accordance with previous observations on protein assemblies.[4a–c]

The simple solution to the above problem is to make use of sparse spin-labeling by diamagnetic dilution of the spin-label reagent with its diamagnetic analog (Figure 1 C), in our case MTSL (1-oxyl-2,2,5,5-tetramethyl-δ3-pyrroline-3-methyl methanethiosulfonate) and MTS (1-acetoxy-2,2,5,5-tetramethyl-δ3-pyrroline-3-methyl methanethiosulfonate),[14] respectively. Alternatively one can reduce the ratio of spin-label reagent to free cysteines (SI Figure S2). In both instances, as the fractional MTSL labeling is reduced, the decay rate and amplitude of the slow component of the phase memory relaxation are increased, while the amplitude of the fast component is concomitantly reduced even though its decay rate is unaffected (Figure 2 A and Table 1, and SI Figure S2 and Table S1).

To observe dipolar coupling at least 2 sites (out of 14 in GroEL) must be labelled, but labeling of more than 2 sites decreases the T_m. Thus the ratio of MTSL to MTS needs to be optimized to minimize the fraction of GroEL labeled at only a single site or at more than 2 sites. A 1:7 ratio of MTSL:MTS would result in the largest fraction of GroEL molecules

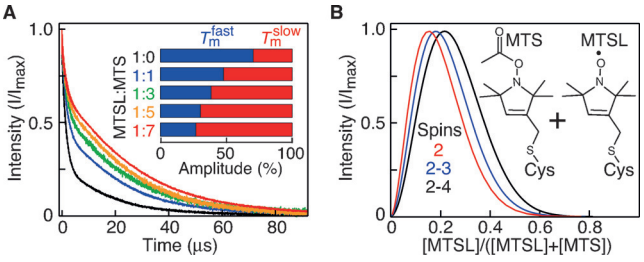

Figure 2. Impact of fractional spin-labeling on the phase memory time T_m. A) Q-band spin-echo decay curves for fully deuterated GroEL-(E315C) showing the increase in T_m accompanying a reduction in the number of spin-labeled subunits obtained by diluting MTSL through the introduction of its diamagnetic analog MTS (since the probability of a surface exposed cysteine being labelled with MTSL or MTS is essentially the same).[13] B) Probability of labeling 2 (red), 2 to 3 (blue) and 2 to 4 (black) subunits of GroEL as a function of the fractional population of MTSL given by [MTSL]/([MTSL]+[MTS]). The pulse sequence employed to acquire the spin-echo decay curves in panel (A) was a standard two-pulse Hahn echo experiment with the echo signal recorded as a function of the echo delay time with time steps of 20 ns up to a total evolution time of 90 µs, limited by the traveling-wave tube amplifier. The length of the π/2 pulse was 12 ns, the shot repetition time was set to 20 ms, and the pulse gate time used for echo integration was 32–38 ns. All Q-band (33.8 GHz) data in this paper were acquired on a Bruker E-580 spectrometer equipped with a 150 W traveling-wave tube amplifier, a model ER5107D2 resonator, and a cryofree cooling unit operating at 50 K. Sample conditions here and throughout the paper were 50 µM spin-labeled, fully deuterated GroEL 14mer, 10 mM Tris pH 8, 20 mM $MgCl_2$, 30 %/70 % (*v*/*v*) [D_8]glycerol/D_2O.

Table 1: Effect of sparse spin-labeling on the decay rates (T_m) and amplitudes (A) of the fast and slow components of phase memory relaxation for fully deuterated spin-labeled GroEL(E315C) at 50 K.[a]

[MTSL]:[MTS]	T_m^{fast} [µs]/A_{fast} [%]	T_m^{slow} [µs]/A_{slow} [%]
1:0	1.5 ± 0.1/70.4 ± 0.1	18.4 ± 0.1/29.6 ± 0.1
1:1	1.4 ± 0.1/47.9 ± 0.1	21.3 ± 0.1/52.1 ± 0.1
1:3	1.4 ± 0.1/38.5 ± 0.1	24.6 ± 0.1/61.5 ± 0.1
1:5	1.2 ± 0.1/30.4 ± 0.1	23.8 ± 0.1/69.6 ± 0.1
1:7	1.2 ± 0.1/26.9 ± 0.1	26.9 ± 0.1/73.1 ± 0.1

[a] For GroEL(R268C) spin-labeled at a 1:5 ratio of MTSL to MTS, T_m^{fast} and T_m^{slow} have values of 2.3 ± 0.2 and 21.6 ± 0.1 µs, respectively, with corresponding amplitudes of 49.6 ± 0.2 and 50.4 ± 0.1 %. The lower amplitude for the slow component relative to that for GroEL(E315C) under the same labeling conditions may be due to the presence of some very short (ca. 15 Å) distances between spin labels giving rise to strong dipolar coupling (cf. Figure 1 A).[6]

occupied by two spin labels but would also result in a significant fraction of GroEL molecules with only a single spin label which would not contribute to the DEER dipolar evolution curve. Thus, we decided to use a ratio of MTSL to MTS (ca. 1:5 in this instance) that results in the largest fraction of molecules with 2 to 3 spin labels (Figure 2B), reducing the one-spin label species while still retaining a large amplitude for T_m^{slow} (Figure 2A and Table 1), and a modulation depth in excess of 50% (SI Figure S3). The presence of some species containing three spin labels will be associated with "ghost" peak contributions to the $P(r)$ distance distributions which can be minimized by reducing the normalized modulation depth (Δ/Δ_{180}) to a value of ca. 0.6 by decreasing the ELDOR pump pulse flip angle from the usual 180° to 60–70°.[6b]

Q-band DEER echo curves recorded on fully deuterated GroEL(R268C) and GroEL(E315C), spin-labeled using a ratio of 1:5 MTSL to MTS, with different t_{max} values (20 and 35 µs for the R268C sample, and 47 and 80 µs for the E315C sample) are shown in Figure 3A (left and right panels, respectively). For comparison a DEER echo curve recorded with a t_{max} of 18 µs is included for fully spin-labeled and deuterated GroEL(E315C), highlighting the resulting very rapid signal decay and the huge gains afforded by sparse spin-labeling. $P(r)$ distributions derived from the DEER echo curves using the programs DD[14] and DeerAnalysis[15] are shown in Figure 3B. The former makes use of a mathematical model (in this instance a sum of Gaussians) to directly fit the DEER data (including automated background subtraction with a best-fit exponential decay), while the latter is model free and uses Tikhonov regularization. The predicted $P(r)$ distributions derived from the apo GroEL crystal structure[8] using MMMv2013.2[10] are shown by the grey envelopes. For GroEL(R268C) the predicted intra-ring distances between spin labels fall into two classes comprising two distances around 15 Å, and four distances that coalescence into a broad distribution centered at 37 Å; the seven predicted intra-ring distances merge into a single distribution centred around

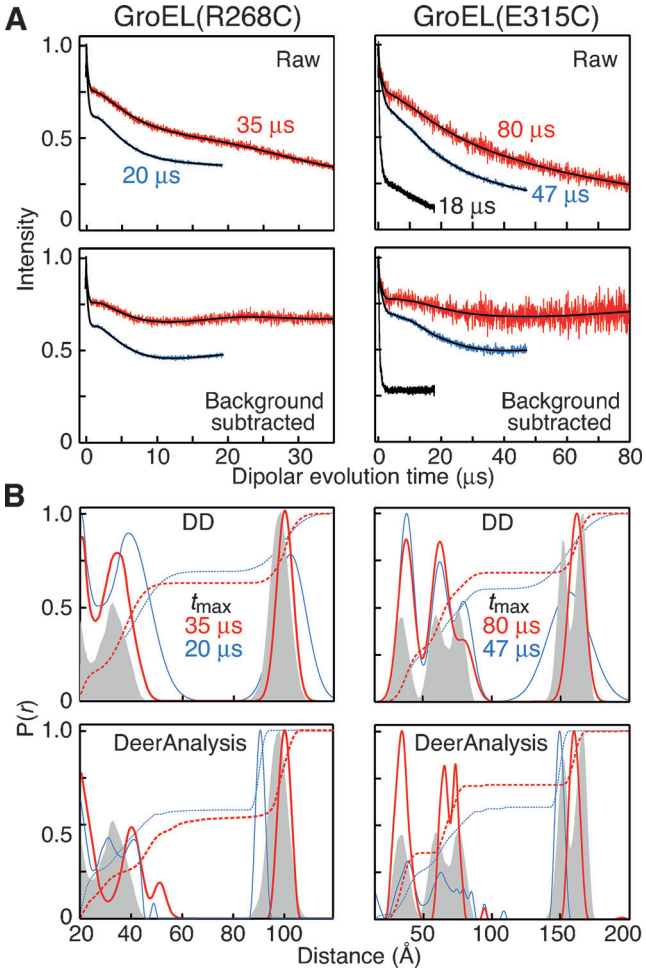

Figure 3. Q-band DEER measurements on fully deuterated GroEL. A) Raw (upper panels) and background subtracted (lower panels) Q-band four-pulse DEER[1d] echo curves recorded at 50 K on GroEL-(R268C) (left panels) and GroEL(E315C) (right panels). Optimized nitroxide spin-labeling to maximize the GroEL molecules with either 2 or 3 spin labels was obtained using a 1:5 ratio of MTSL to MTS (red and blue DEER echo curves); for comparison a DEER echo curve obtained on a sample of GroEL(E315C) with 100% spin-labeling is shown in black (right panel). The DEER dipolar evolution curves shown in red (t_{max} = 35 and 80 µs, for the R268C and E315C samples, respectively) were obtained with flip angle reduction[6b] to minimize dipolar truncation: the ELDOR pulse flip angles (θ) were set to 72 and 64°, respectively, corresponding to normalized modulation depths ($\Delta_\theta/\Delta_{\theta=180°}$) of 0.59 and 0.62, respectively. The DEER dipolar evolution curves shown in blue (t_{max} = 20 and 47 µs for the R268C and E315C samples, respectively) were obtained using an ELDOR pulse flip angle of 180°. No ELDOR pulse flip angle reduction was used for the black curve (left panel). B) $P(r)$ distance distributions derived from the DEER echo curves (color coding as in panel (A)) using the programs DD[14] and DeerAnalysis 2013[15] (top and bottom panels, respectively). The integrals of the $P(r)$ distributions are shown as dashed lines, and the grey envelopes indicate the predicted $P(r)$ distributions derived from the apo GroEL crystal structure (PDB 1XCK)[8] using the program MMMv2013.2.[10] Good agreement is seen between the experimental and theoretical $P(r)$ distributions. In the case of DeerAnalysis, L-curves were used to select the optimal Tikhonov regularization parameter α which was set to a value of 1000. The best-fit DEER echo curves calculated from the DD analysis are shown as thin black lines in panel (A). The background function used by DD is an exponential with a best-fit decay rate (see SI Figure S4). The long 160 Å inter-ring distance for GroEL(E315C) cannot be extracted from the DEER curve recorded on fully spin-labeled and deuterated GroEL(E315C) acquired with a t_{max} value of 18 µs (black traces in the right-hand panels of (A)) as shown in SI Figure S5. The observe and ELDOR pump pulses used for the DEER evolution curves were separated by 90 MHz with the observe $\pi/2$ and π pulses set to 12 and 24 ns, respectively. The ELDOR pulse length was set to 8 ns and the flip angle adjusted by appropriate attenuation. The pump frequency was centred at the Q-band nitroxide spectrum located at +40 MHz from the centre of the resonator frequency. The τ_1 value for the first echo-period time of 400 ns was incremented eight times in 16 ns steps to average ^{2}H modulation; the position of the ELDOR pump pulse was incremented in steps Δt = 20, 40 and 60 ns for fully spin-labeled GroEL(E315C), sparsely-labeled GroEL(R268C) and sparsely-labeled GroEL(E315C), respectively. The bandwidth of the overcoupled resonator was 120 MHz. The second echo period time τ_2 was set t_{max} + 700 ns; data collection was not extended to the full τ_2 range because of a persistent "2 + 1" echo perturbation of the DEER echo curves at a time of about τ_1 from the final observe π pulse. The pulse gate time used for echo integration was 32–38 ns. Total acquisition time was 24 hours for the shorter t_{max} values, and 4 days for the t_{max} = 80 µs data.

100 Å. For GroEL(E315C), the six intra-ring distances fall into three resolved distributions centred at 35, 60 and 78 Å, while the inter-ring distances which range from 146–170 Å, fall into two classes centred at 152 and 162 Å. Overall, for both GroEL(R268C) and GroEL(E315C), the $P(r)$ distributions derived from the DEER data recorded with the longer t_{max} (red curves; 35 μs for R268C and 80 μs for E315C), using either DD[14] or DeerAnalysis[15] (Figure 3B, top and bottom panels, respectively), match closely with the predicted distributions from the crystal structure, reflecting the increased accuracy afforded by extending the measurement to longer dipolar evolution times.

A summary of the intra- and inter-ring mean distances between spin labels derived from the long t_{max} DEER data using DD[14] and DeerAnalysis[15] is provided in Table 2. The long inter-ring mean distances, 103 and 160 Å for GroEL-(R268C) and GroEL(E315C), respectively, obtained by the

Table 2: Mean distances between spin labels derived from DEER data acquired with long dipolar evolution times.[a]

GroEL construct	Distance [Å] DD[b,c]	DeerAnalysis[c]
R268C	36	39
	–	52
	103	104
E315C	39	35
	63	66
	81	74
	160	160

[a] t_{max} = 35 μs from GroEL(R268C) and 80 μs for GroEL(E315C). [b] The number of Gaussians used in the DD fits was assessed using the Akkaike information criterion[16] corrected for finite sample size (with the optimal number of Gaussians required to represent the data identified by the lowest Akaike value): 3 Gaussians were used for the GroEL(R268C) data and 4 for the GroEL(E315C) data. [c] The lower limit of accessible distances was set to 20 Å for the GroEL(R268C) data and 15 Å for the GroEL(E315C) data.

two methods of analysis are in excellent agreement with one another. The same is approximately true for the three shorter intra-ring mean distances obtained for GroEL(E315C). The intra-ring distances for GroEL(R268C) are well reproduced from the DD analysis, but appear to be shifted to slightly higher values with DeerAnalysis. This may be due the fact that DD describes the DEER echo curve for GroEL(R268C) as a function of three Gaussians, while no assumption on the number of distances is made by the model free DeerAnalysis approach. The unconstrained nature of the latter, particularly when the data at short dipolar evolution times are under-sampled (since we were basically interesting in measuring the longer distances beyond 100 Å), may result in potential overfitting of the data, accounting for both the shifts in peak positions and possibly the appearance of a longer distance at around 50 Å.

The total integrated intensities for the long inter- and short intra-ring $P(r)$ distance distributions should in principle be roughly comparable given that there are 6 intra- and 7 inter-ring distances. This is approximately true for GroEL-(R268C), but not for GroEL(E315C) where the integrated intensity of the long inter-ring distances centered around 160 Å is clearly underestimated (Figure 3B). This is due to the fact that the value of t_{max} (in μs) required to measure an accurate mean distance (r_m in Å) is given by $2(r_m/50)^3$ μs, but the value required to accurately determine both mean distance and distribution width (and hence integrated intensity) is given by $2(r_m/40)^3$ μs.[2c] The latter condition is satisfied with t_{max} = 35 μs for the 103 Å mean distance in GroEL-(R268C), but not with t_{max} = 80 μs for the 160 Å mean distance in GroEL(E315C) where a t_{max} value of $\geq$130 μs would be required.

In conclusion, distances between nitroxide spin labels in the 100 to 170 Å range are accessible to DEER in symmetric multimeric proteins using sparse spin-labeling to increase both the length (ca. 1.5-fold) and amplitude (3 to 3.5-fold) of the slow component of phase memory relaxation, over and above what is already achievable by full deuteration of protein and solvent. As a result DEER echo curves can be acquired for long dipolar evolution times up to a t_{max} of ca. 80 μs which corresponds to an upper mean distance limit of ca. 170 Å.[2c] This approach, which is easy to implement by simply controlling the ratio of nitroxide spin-label to diamagnetic analog, should find wide applicability for the study of conformational changes involving many multimeric systems, including an array of molecular machines, ion transporters and transmembrane assemblies.

Acknowledgements

This work was supported by funds from the Intramural Research Program of NIDDK, NIH, and from the Intramural AIDS Targeted Antiviral Program of the Office oft he Director of the NIH (to G.M.C.).

Keywords: biophysics · chemical physics · EPR spectroscopy · spectroscopic methods · structural biology

How to cite: *Angew. Chem. Int. Ed.* **2016**, *55*, 15905–15909
Angew. Chem. **2016**, *128*, 16137–16141

[1] a) A. D. Milov, K. M. Salikhov, M. D. Shirov, *Fiz. Tverd. Tela* **1981**, *23*, 975–982; b) A. D. Milov, A. B. Ponomarev, Y. D. Tsvetkov, *Chem. Phys. Lett.* **1984**, *110*, 67–82; c) R. G. Larsen, D. J. Singel, *J. Chem. Phys.* **1993**, *98*, 5134–5146; d) M. Pannier, S. Veit, A. Godt, G. Jeschke, H. W. Spiess, *J. Magn. Reson.* **2000**, *142*, 331–340.

[2] a) G. Jeschke, Y. Polyhach, *Phys. Chem. Chem. Phys.* **2007**, *9*, 1895–1910; b) C. Altenbach, A. K. Kusnetzow, O. P. Ernst, K. P. Hofmann, W. L. Hubbell, *Proc. Natl. Acad. Sci. USA* **2008**, *105*, 7439–7444; c) G. Jeschke, *Annu. Rev. Phys. Chem.* **2012**, *63*, 419–446.

[3] a) G. Jeschke, *ChemPhysChem* **2002**, *3*, 927–932; b) R. Ward, A. Bowman, E. Sozudogru, H. El-Mkami, T. Owen-Hughes, D. G. Norman, *J. Magn. Reson.* **2010**, *207*, 164–167; c) A. Bowman, C. M. Hammond, A. Stirling, R. Ward, W. Shang, H. El-Mkami, D. A. Robinson, D. I. Svergun, D. G. Norman, T. Owen-Hughes, *Nucleic Acids Res.* **2014**, *42*, 6038–6051; d) H. El Mkami, D. G. Norman, *Methods Enzymol.* **2015**, *564*, 125–152.

[4] a) G. Hagelueken, W. J. Ingledew, H. Huang, B. Petrovic-Stojanovska, C. Whitfield, H. ElMkami, O. Schiemann, J. H. Naismith, *Angew. Chem. Int. Ed.* **2009**, *48*, 2904 – 2906; *Angew. Chem.* **2009**, *121*, 2948 – 2950; b) D. T. Edwards, T. Huber, S. Hussain, K. M. Stone, M. Kinnebrew, I. Kaminker, E. Matalon, M. S. Sherwin, D. Goldfarb, S. Han, *Structure* **2014**, *22*, 1677 – 1686; c) S. Valera, K. Ackermann, C. Pliotas, H. Huang, J. H. Naismith, B. E. Bode, *Chemistry* **2016**, *22*, 4700 – 4703; d) A. Giannoulis, R. Ward, E. Branigan, J. H. Naismith, B. E. Bode, *Mol. Phys.* **2013**, *111*, 2845 – 2854; e) B. Endeward, J. A. Butterwick, R. MacKinnon, T. F. Prisner, *J. Am. Chem. Soc.* **2009**, *131*, 15246 – 15250.

[5] a) H. Sato, V. Kathirvelu, G. Spagnol, S. Rajca, A. Rajca, S. S. Eaton, G. R. Eaton, *J. Chem. Phys. B* **2008**, *112*, 2818 – 2828; b) H. Sato, S. E. Bottle, J. P. Blinco, A. S. Micallef, G. R. Eaton, S. S. Eaton, *J. Magn. Reson.* **2008**, *191*, 66 – 77.

[6] a) G. Jeschke, M. Sajid, M. Schulte, A. Godt, *Phys. Chem. Chem. Phys.* **2009**, *11*, 6580 – 6591; b) T. von Hagens, Y. Polyhach, M. Sajid, A. Godt, G. Jeschke, *Phys. Chem. Chem. Phys.* **2013**, *15*, 5854 – 5866.

[7] D. Thirumalai, G. H. Lorimer, *Annu. Rev. Biophys. Biomol. Struct.* **2001**, *30*, 245 – 269.

[8] C. Bartolucci, D. Lamba, S. Grazulis, E. Manakova, H. Heumann, *J. Mol. Biol.* **2005**, *354*, 940 – 951.

[9] G. G. Krivov, M. V. Shapovalov, R. L. Dunbrack, Jr., *Proteins* **2009**, *77*, 778 – 795.

[10] Y. Polyhach, E. Bordignon, G. Jeschke, *Phys. Chem. Chem. Phys.* **2011**, *13*, 2356 – 2366.

[11] E. J. Hustedt, R. A. Stein, L. Sethaphong, S. Brandon, Z. Zhou, S. C. Desensi, *Biophys. J.* **2006**, *90*, 340 – 356.

[12] J. L. Baber, J. M. Louis, G. M. Clore, *Angew. Chem. Int. Ed.* **2015**, *54*, 5336 – 5339; *Angew. Chem.* **2015**, *127*, 5426 – 5429.

[13] A. Gross, L. Columbus, K. Hideg, C. Altenbach, W. L. Hubbell, *Biochemistry* **1999**, *38*, 10324 – 10335.

[14] S. Brandon, A. H. Beth, E. J. Hustedt, *J. Magn. Reson.* **2012**, *218*, 93 – 104.

[15] G. Jeschke, V. Chechik, P. Ionita, A. Godt, H. Zimmerman, J. E. Banham, C. R. Timmel, D. Hilger, H. Jung, *Appl. Magn. Reson.* **2006**, *30*, 473 – 498.

[16] R. A. Stein, A. H. Beth, E. J. Hustedt, *Methods Enzymol.* **2015**, *563*, 531 – 567.

Manuscript received: September 30, 2016
Final Article published: November 17, 2016

